Polarized hyper-Rayleigh light scattering measurements of nonlinear optical chromophores

Philip Kaatz and David P. Shelton
Department of Physics, University of Nevada Las Vegas, Las Vegas, Nevada 89154-4002

(Received 15 April 1996; accepted 5 June 1996)

Hyper-Rayleigh light scattering measurements at incident wavelengths of 1064 and 1319 nm are reported for several organic nonlinear optical chromophores in solution with approximately 5%–10% uncertainty in the relative first hyperpolarizabilities. The measured chromophores include representatives from C_1, C_s, C_{2V}, and D_3 molecular point groups and include both neutral and ionic compounds. The measurements were made with 2–5 cm^{-1} spectral resolution and include polarization analysis of the incident and scattered light. Polarization ratios were measured with 2%–3% uncertainty for each molecule, and relative magnitudes of the hyperpolarizability components were deduced. Two-photon induced fluorescence from several chromophores was observed to overlap with the scattered second harmonic light spectrum. The use of a scanning monochromator, however, generally allows the separation of these two sources of photons. The measured first hyperpolarizabilities are consistent with previous electric field induced second harmonic generation measurements of the same compounds, provided that the standard reference value for the nonlinear susceptibility of quartz is taken to be $d_{11}=0.30\pm0.02$ pm/V at 1064 nm.
 [S0021-9606(96)52234-8]

I. INTRODUCTION

Until recently, the only method in widespread use for measuring the second order nonlinear optical (NLO) properties of organic molecules was the electric field induced second harmonic generation (EFISHG) experiment. Due to the use of a static electric field in this experiment, the compounds investigated by the EFISHG method are restricted to neutral dipolar species. As other authors have indicated, there exist many potentially interesting molecules whose NLO properties cannot be assessed by this experiment because of symmetry constraints or because they exist as ionic species.[1,2] The quantity measured in the EFISHG experiment is proportional to[3]

$$\left(\gamma+\frac{\mu\beta_z}{5kT}\right), \tag{1}$$

where the first and second hyperpolarizabilities are given by β and γ. The molecular dipole moment is μ and the projection of β in the direction of the dipole moment is given by β_z. T is the temperature, with k Boltzmann's constant. This experiment requires an extensive set of physical and optical measurements characterizing the density, refractive index, dielectric constant, and EFISHG amplitudes and coherence lengths on a series of solutions of graded concentration.[4] For accurate work, additional third harmonic or other measurements assessing the magnitude of the second hyperpolarizability are required in order to obtain the first hyperpolarizabilities of the compounds.[5] Temperature dependent EFISHG studies provide an accurate separation of the first and second hyperpolarizabilities, however, such measurements are only feasible in the gas phase.[6] In contrast, the hyper-Rayleigh scattering (HRS) experiment is dependent only upon β and requires only an efficient detection system to collect the scattered second harmonic light.

In spite of the seemingly simple experimental requirements of the HRS apparatus, the results obtained by the HRS method have occasionally been significantly different than those obtained by the EFISHG experiment (when a direct comparison is possible). In particular, for compounds such as *N*,*N*-dimethylaminonitrostilbene (DANS), the NLO properties are expected to be essentially one dimensional and the two NLO characterization methods are expected to yield equivalent results. It has become apparent that the anomalous HRS results are due to two-photon induced fluorescence from some of these molecules.[7–9] The presence of this two-photon induced fluorescence overlaps with the HRS spectrum and has prevented the previous authors from making an accurate assessment of the scattered second harmonic intensity. With the use of a scanning monochromator in the HRS apparatus to isolate the second harmonic signal, we find that consistent results are obtained from the HRS method and the EFISHG experiment for a determination the molecular β of these compounds. Calibration of the absolute β values was accomplished with respect to a HRS measurement of carbon tetrachloride, which has been previously characterized.[10] Except for measurements on molecular liquids,[10–13] previous HRS measurements have not provided any spectral information, as the spectral selectivity was achieved with interference filters.

The polarization of the incident and scattered light is analyzed in this work. As all components of the hyperpolarizability tensor β can contribute to HRS, detailed polarization studies of the sample are able to provide information on several components of β. We provide expressions for the HRS for several molecular point groups assuming elliptically polarized incident light and detection of the second harmonic scattered light at 90° to the input light. These expressions provide a means of assessing the relative magnitudes of the

 0021-9606/96/105(10)/3918/12/$10.00

TABLE I. Chromophore acronyms.

pNA: *p*-Nitroaniline
oMA: *o*-Nitroaniline
mNA: *m*-Nitroaniline
DAB: 4-Dimethylaminobenzaldehyde
MNA: 2-Methyl, 4-nitroaniline
DAC: 4-Dimethylaminocinnamaldehyde
MK: (Michler's Ketone) 4,4′ Bis(dimethylamino)benzophenone
DBCP: 2,5 Dibenzylidenecyclopentanone
BDABA: trans, trans-Bis[4-(dimethylamino)benzylidene]acetone
DABMN: Dimethylaminobenzylidenemalononitrile
DANS: 4-(Dimethylamino)-4′-nitrostilbene
Coumarin 334: 2,3,5,6 1H,4H-Tetrahydro-9-acetylquinolizino-[9,9a,1-*gh*]-coumarin
DCM: 4-Dicyanmethylene-2-methyl-6-(*p*-dimethylaminostyryl)-4H-pyran
DR1: (Disperse Red 1) 4-[N-ethyl-N-(2-hydroxyethyl)] amino-4′-nitroazobenzene
LDS 722: 1-Ethyl-4(4-(*p*-Dimethylaminophenyl)-1,3-butadienyl)-pyridinium Perchlorate
Styryl 7: 2-[4-(4-dimethylaminophenyl)-1,3-butadienyl]-3-ethyl-benzothiazolium *p*-toluene sulfonate
DIA: N,N Dimethylindoaniline
RB (Rhodamine B): 2-[6-Diethylamino)-3-(diethylamino)-3H-xanthen-9-yl] benzoic acid
CV: Crystal Violet
BG: Brilliant Green
BTB: Bromothymol Blue

first hyperpolarizability components that are needed for an accurate assessment of β from HRS measurements. We conclude that HRS measurements are capable of the same or better level of accuracy as EFISHG measurements, with the benefit of being able to probe a wider variety of molecules and different hyperpolarizability components.

II. EXPERIMENT

The molecules investigated in this work are listed in Table I. All compounds were obtained from Aldrich Chemical except for DANS, which was purchased from Acros Chemical (a division of Fisher Scientific) and LDS 722, which was purchased from Exciton, Inc.. The purity of the compounds was typically greater than 95% and they were used as received. All the compounds were prepared as dilute solutions in 1,4 dioxane, which has negligible HRS signal for all polarization geometries. Approximately 5% methanol was added to the solutions of the molecular salts to aid in the dissolution of these compounds. Normal 1 cm spectroscopic fused silica cuvettes were used for measurements and in typical experiments a 1.0 cm^3 volume of liquid was sufficient. The solutions were filtered through a 0.2 μm micropore filter to remove dust particles that could be a source of spurious second harmonic signal. When comparing chromophores in different solvents, the second harmonic signal was corrected for the effects of thermal lensing. The maximal HRS signal was limited due to strong thermal lensing from absorption at 1064 or 1319 nm by a C–H vibrational overtone.

A schematic diagram of the experimental apparatus is shown in Fig. 1. The incident radiation at 1064 or 1319 nm was obtained from an acousto-optically *Q*-switched Nd:YAG laser (Quantronix 116) operating in a near Gaussian TEM_{00} mode with a measured $M^2 \approx 1.1$. The laser produced trains of ≈150 ns, 1 mJ pulses at a repetition rate of 3 kHz at 1064 nm and ≈400 ns, 0.1 mJ pulses at a repetition rate of 1 kHz at 1319 nm. The input power level and polarization were selected by two Glan–Laser polarizers followed by a Soleil–Babinet compensator. The incident laser beam was focused into the sample cell with a 4X microscope objective lens (focal length 32 mm) and positioned to pass at a distance of 2 mm from the inside of the cell wall facing the collecting lens. The scattered light was collected at 90° with $f/1.8$ optics and focused into a spectrometer (Jobin–Yvon Ramanor U 1000), with polarization selection by a sheet polaroid. The relative spectral response of the complete spectrometer was calibrated with respect to the graybody radiation emitted from a tungsten filament lamp, see Fig. 2. The entrance slits of the spectrometer were closed to provide a spectral slit width of 2–5 cm^{-1}. The spectrally dispersed light was detected by a cooled photon counting photomulti-

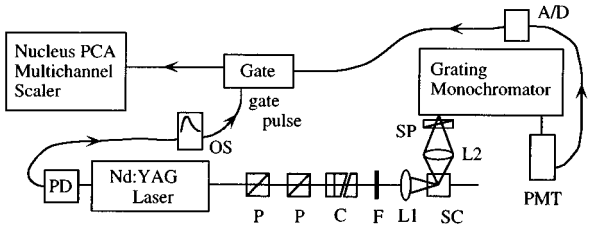

FIG. 1. Experimental setup for spectral measurements of hyper-Rayleigh light scattering. The components are denoted by: P: Glan-Laser Polarizer; C: Soleil-Babinet Compensator; F: RG 850 Filter; L1: 4 X Microscope Objective; L2: 50 mm Camera Lens; PD: Photodiode; SC: Sample Cell; SP: Sheet Polarizer; OS: Oscilloscope; PMT: Photomultiplier Tube; A/D: Amplifier/Discriminator.

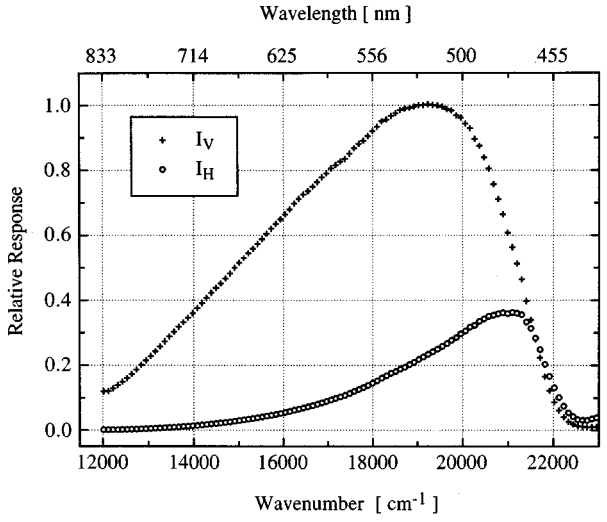

FIG. 2. Relative response (relative detection probability for a photon) of the Jobin-Yvon Ramanor U 1000 spectrometer for vertically (I_V) and horizontally (I_H) polarized light entering the spectrometer. The relative response also includes losses due to the analyzer, the collecting optics, and the PMT spectral response. The spectrometer was calibrated with respect to the graybody radiation emitted from a tungsten filament lamp.

plier tube (Hamamatsu R943) which was followed by an amplifier/discriminator. The output pulses corresponding to individual detected photons were counted by a multichannel scaler (Nucleus PCA). More details of the experimental apparatus have been given in a previous communication.[13]

III. THEORY

Hyper-Rayleigh or second harmonic light scattering denotes a process in which two photons of frequency ω incident upon a noncentrosymmetric molecule or ensemble of molecules are absorbed and simultaneously a third photon of frequency 2ω is emitted. The nonlinear optical response of an isolated molecule irradiated with light of high intensity is usually written as a Taylor series expansion of the induced dipole moment μ in terms of the applied electric field $E_i(\omega)$,

$$\mu_i = \alpha_{ij}E_i + \frac{1}{2}\,\beta_{ijk}E_iE_j + \cdots\,, \tag{2}$$

where the molecular tensors α and β describe the linear and lowest order nonlinear optical properties of the molecules, respectively. Note, that many experimentalists, especially those using the EFISHG technique, use a series expansion of the induced dipole moment without the factors of $1/n!$ in the definitions of the molecular hyperpolarizabilities. If the incident light is assumed to be travelling in the **x** direction, the polarization of the incident electric field, $\mathbf{E}(\omega)$, can be described by the following equation:

$$\mathbf{E}(\omega) = E_0\{\cos\,\psi\,\cos\,\omega t\,\mathbf{e}_y + \sin\,\psi\,\cos(\omega t+\delta)\mathbf{e}_z\}, \tag{3}$$

where ψ and δ are arbitrary angles. Circularly polarized light is described by $\psi=\pi/4$ and $\delta=\pi/2$ and linearly polarized light by $\psi=0$ (horizontal) or $\psi=\pi/2$ (vertical).

The second harmonic light intensity for a collection of N noninteracting molecules without orientational correlations is given by $I^{2\omega} \propto N\langle\mu_i(2\omega)\mu_i^*(2\omega)\rangle$, where the brackets indicate averaging over all possible molecular orientations. The total intensity is simply the sum of the intensities scattered by the individual molecules because the phase of the scattered light, which depends on the orientation of the molecule, varies randomly from one molecule to the next. The ensemble averaging over the molecular motions indicated by the brackets will involve products of components of the first hyperpolarizability tensor β of the form $\langle\beta_{IJK}\beta_{LMN}\rangle$. Assuming the scattered HRS signal is collected at 90° along the **y** direction, the polarization dependence of the second harmonic signal is given by[14]

$$\begin{aligned} I_{EV}^{2\omega} \propto \langle\mu_z^2\rangle \propto \langle\beta_{ZYY}^2\rangle\cos^4\,\psi + \langle\beta_{ZZZ}^2\rangle\sin^4\,\psi \\ + \sin^2\,\psi\,\cos^2\,\psi\langle(\beta_{ZYZ}+\beta_{ZZY})^2 \\ + 2\beta_{ZZZ}\beta_{ZYY}\,\cos\,2\delta\rangle, \end{aligned} \tag{4a}$$

$$\begin{aligned} I_{EH}^{2\omega} \propto \langle\mu_x^2\rangle \propto \langle\beta_{XZZ}^2\rangle\sin^4\,\psi + \langle\beta_{XYY}^2\rangle\cos^4\,\psi \\ + \sin^2\,\psi\,\cos^2\,\psi\langle(\beta_{XYZ}+\beta_{XZY})^2 \\ + 2\beta_{XZZ}\beta_{XYY}\,\cos\,2\delta\rangle, \end{aligned} \tag{4b}$$

$$\begin{aligned} \langle\mu_y^2\rangle \propto \langle\beta_{YYY}^2\rangle\cos^4\,\psi + \langle\beta_{YZZ}^2\rangle\sin^4\,\psi \\ + \sin^2\,\psi\,\cos^2\,\psi\langle(\beta_{YZY}+\beta_{YYZ})^2 \\ + 2\beta_{YYY}\beta_{YZZ}\,\cos\,2\delta\rangle, \end{aligned} \tag{4c}$$

where the subscripts V, H, and E indicate vertically, horizontally, and elliptically polarized light, respectively. The macroscopic averages $\langle\beta_{IJK}\beta_{LMN}\rangle$ are quadratic forms of the microscopic molecule-fixed-axis hyperpolarizability components, β_{ijk}. These products may be calculated for molecules of any point group by using, for example, Table I and Eqs. (34)–(44) of Bersohn *et al.*[14] or Table II and Eqs. (11)–(13) from Cyvin *et al.*[15] In the general case, assuming that the first hyperpolarizability tensor is real, at most five invariants of the molecular hyperpolarizabilities may be determined, depending upon the molecular symmetry. Consequently, elliptically polarized light is required to obtain full information on these invariants when the detected scattered harmonic light is restricted to be linearly polarized. Subsequent work has shown that other polarization geometries may be required if the first hyperpolarizability tensor has an imaginary component.[16,17]

A Soleil–Babinet compensator is used in our apparatus to create elliptically polarized light from the incident horizontally polarized light. The polarization of the light leaving the compensator can be written as[13,18]

$$\mathbf{E}(\omega) = E_0(\omega)\left\{\cos\,\frac{\Gamma}{2}\,\mathbf{e}_H - i\,\sin\,\frac{\Gamma}{2}\,\mathbf{e}_V\right\}. \tag{5}$$

This is equivalent to the polarized light described by Eq. (3) provided that $\delta=\pi/2$ and $\psi=\Gamma/2$. The standard VV and VH polarization geometries in Eqs. (4a) and (4b) correspond to setting the retardation of the compensator to $\Gamma=2\psi=\pi$, and selecting V or H with the appropriate setting of the analyzer. Similarly, the HV and HH scattering geometries are obtained from $\Gamma=2\psi=0$, with $\delta=\pi/2$ and the V or H setting of the analyzer.

As the HRS scattered light is collected at $f/1.8$ from the scattering source, the polarization is averaged over the solid angle around the nominal 90° scattering geometry.[13] The polarization ratios were corrected for the effect of a finite collection angle θ_0, and the reported polarization ratios are the values that would be obtained for $\theta_0=0$. The scattering geometries VH and HV are not equivalent except at $\theta_0=0$. At $f/1.8$, the corrections to $I_{\mathrm{VV}}^{2\omega}/I_{\mathrm{VH}}^{2\omega}$ are always less than 1.5%, but corrections to $I_{\mathrm{VV}}^{2\omega}/I_{\mathrm{VH}}^{2\omega}$ are as large as 9% when $I_{\mathrm{VV}}^{2\omega}/I_{\mathrm{VH}}^{2\omega}=5$. In our apparatus, the effects of a diverging input beam on the HRS polarization ratios are negligible. With the present optics the focal region of the input beam where the HRS signal is produced has an effective beam divergence $\approx f/30$. In addition, the effects of the input beam divergence add in quadrature to both the effective collection angle and extinction ratio giving a $<0.5\%$ correction to the previously calculated detection solid angle correction to the measured HRS polarization ratios.[13] Experimentally, it was more convenient to make measurements in the vertically polarized collection geometry of the scattered light, as the polarization selectivity of the grating in the monochromator provided

5.0× greater intensity for vertically polarized as compared to horizontally polarized light from harmonic scattering at 1064 nm and 16.3× greater intensity at 1319 nm, as shown in Fig. 2.

The measured HRS intensities are strongly affected by the solution refractive indices, n, as the amount of incident and scattered light passed through the cell will depend strongly upon these values. The transmission coefficient through a cell wall is $T_{\mathrm{L},\omega}=[1-(n_{\mathrm{w}}-n_{\mathrm{L}})^2/(n_{\mathrm{w}}+n_{\mathrm{L}})^2]$, with window, n_{w}, and liquid, n_{L}, refractive indices at frequency ω, and where L=S (sample) or R (reference). Provided the laser focusing lens and the light collection lens are correctly repositioned to account for different focal geometries in different solutions, the relation between the relative HRS signal from the sample and reference is given by[13]

$$\frac{I_{\mathrm{S}}^{2\omega}}{I_{R}^{2\omega}}=\frac{n_{\mathrm{S},\omega}}{n_{R,\omega}}\frac{n_{R,2\omega}^2}{n_{\mathrm{S},2\omega}^2}\frac{T_{\mathrm{S},\omega}^2T_{\mathrm{S},2\omega}}{T_{R,\omega}^2T_{R,2\omega}}\frac{\mathscr{L}_{\mathrm{S},\omega}^4\mathscr{L}_{\mathrm{S},2\omega}^2}{\mathscr{L}_{R,\omega}^4\mathscr{L}_{R,2\omega}^2}\frac{N_{\mathrm{S}}}{N_R}\frac{\langle\beta_{\mathrm{S}}^2\rangle}{\langle\beta_R^2\rangle}, \tag{6}$$

where the factors account for effective scattering source length, collection solid angle, reflection losses, local fields, sample number density, and molecular hyperpolarizability, in that order. The Lorentz local field for sample S at frequency ω is assumed to be given by $\mathscr{L}_{\mathrm{S},\omega}=(n_{\mathrm{S},\omega}^2+2)/3$. As all the HRS measurements of the chromophores reported in this work [except for a solvent dependence study of p-nitroaniline (pNA), see below] were made under nearly the same solvent conditions (1,4 dioxane), these factors due to the molecular environment are expected to be constant. A standard solution of pNA in 1,4 dioxane served as a secondary external reference standard for the comparison of the harmonic scattering from different NLO chromophores.

The comparison of different chromophores is based on the HRS measurements of the sample solutions in the VV polarization geometry. In this case, the second harmonic intensity of the sample, $I_{\mathrm{VV}}^{2\omega}$, is given by

$$I_{\mathrm{VV}}^{2\omega}\propto N\langle\beta_{ZZZ}^2\rangle(I^{\omega})^2\times10^{-A}, \tag{7}$$

where the absorbance, $A=\epsilon_{2\omega}cl$, accounts for the absorption losses at the second harmonic wavelength (532 or 660 nm). The extinction coefficient is $\epsilon_{2\omega}$, the concentration of the solution is given by c, and the distance from the laser beam to the cell wall is l (2 mm). As the reference and the sample chromophores were measured under nearly the same solvent conditions, the first hyperpolarizability of the sample, $\beta_{\mathrm{VV}}^{\mathrm{S}}$, can be obtained from the following equation:

$$\beta_{\mathrm{VV}}^{\mathrm{S}}=\sqrt{\frac{C_{\mathrm{VV}}^{R}}{C_{\mathrm{VV}}^{\mathrm{S}}}}\sqrt{\frac{I_{\mathrm{VV,S}}^{2\omega}}{I_{\mathrm{VV},R}^{2\omega}}}\sqrt{\frac{N_R}{N_{\mathrm{S}}}}\,\beta_{\mathrm{VV}}^{R}, \tag{8}$$

where the subscript VV indicates the appropriate average of the molecule-fixed coefficient of the first hyperpolarizability in the VV polarization geometry. The coefficient C_{VV} is a numerical factor obtained from the spatial averaging of $\langle\beta_{ZZZ}^2\rangle$. In the next section we calculate these factors for some of the molecular point groups of the chromophores investigated in this work, along with the polarization ratios for elliptically polarized light as given by Eqs. (4a)–(4c).

IV. HRS DEPOLARIZATION RATIOS FOR SELECTED POINT GROUPS

The macroscopic averages $\langle\beta_{IJK}\beta_{LMN}\rangle$ that determine the amount of HRS scattering in Eqs. (4a)–(4c) were calculated by using Eqs. (34)–(44) and Table I of Bersohn *et al.*[14] The nonzero components of β were taken from standard compilations of NLO susceptibility component tables.[19] The coefficients β_{VV} and C_{VV} are then obtained by setting $\psi=\pi/2$ in the equations below for $I_{\psi\mathrm{V}}^{2\omega}$. Some of these polarization ratios and their coefficients have been determined previously for selected polarization geometries.[1,2] However, as noted above, in order to correct for the finite collection angle of the detection optics, complete expressions for the dipole moment averages of $\langle\mu_i^2\rangle$ including their polarization dependences are required for a determination of β by the HRS measurement.

A. Molecules of D_{3h} symmetry

One independent nonzero coefficient, β_{yyy}

$$I_{\psi\mathrm{V}}^{2\omega}\propto\langle\mu_z^2\rangle\propto\frac{8}{35}\,\beta_{yyy}^2\left[1+\frac{5}{3}\cos^2\psi-2\cos^4\psi\right], \tag{9a}$$

$$I_{\psi\mathrm{H}}^{2\omega}\propto\langle\mu_x^2\rangle\propto\frac{16}{105}\,\beta_{yyy}^2[1+\cos^2\psi-\cos^4\psi], \tag{9b}$$

$$\langle\mu_y^2\rangle\propto\frac{16}{105}\,\beta_{yyy}^2\left[1+\frac{7}{2}\cos^2\psi-3\cos^4\psi\right], \tag{9c}$$

$$\frac{I_{\mathrm{VV}}^{2\omega}}{I_{\mathrm{HV}}^{2\omega}}=\frac{3}{2}, \tag{9d}$$

$$\beta_{\mathrm{VV}}=\beta_{yyy}\quad\text{and}\quad C_{\mathrm{VV}}=\frac{8}{35}. \tag{9e}$$

B. Molecules of T_d symmetry

One independent nonzero coefficient, β_{xyz}

The equations obtained from Eqs. (4a)–(4c) for molecules of T_d symmetry have been given previously.[13] The results are the same as for molecules of D_{3h} symmetry, with

$$\frac{I_{\mathrm{VV}}^{2\omega}}{I_{\mathrm{HV}}^{2\omega}}=\frac{3}{2}, \tag{10a}$$

but with the exception that

$$\beta_{\mathrm{VV}}=\beta_{xyz}\quad\text{and}\quad C_{\mathrm{VV}}=12/35. \tag{10b}$$

C. Molecules of D_3 symmetry

Two independent nonzero coefficients, β_{xxx} and β_{xyz}

$$I_{\psi\mathrm{V}}^{2\omega}\propto\langle\mu_z^2\rangle\propto\frac{8}{35}\,\beta_{xxx}^2\left[1+\left(\frac{5}{3}+\frac{7}{6}\,R^2\right)\cos^2\psi-2\cos^4\psi\right], \tag{11a}$$

$$I^{2\omega}_{\psi H} \propto \langle \mu_x^2 \rangle \propto \frac{16}{105}\beta^2_{xxx}\left[1+\frac{7}{4}R^2+(1+7R^2)\cos^2\psi - (1+7R^2)\cos^4\psi\right], \tag{11b}$$

$$\langle \mu_y^2 \rangle \propto \frac{16}{105}\beta^2_{xxx}\left[1+\left(\frac{7}{2}+\frac{7}{4}R^2\right)\cos^2\psi - \left(3+\frac{7}{4}R^2\right)\cos^4\psi\right], \tag{11c}$$

$$\frac{I^{2\omega}_{VV}}{I^{2\omega}_{HV}} = \frac{6}{4+7R^2}, \tag{11d}$$

where $R=\beta_{xyz}/\beta_{xxx}$ and

$$\beta_{VV}=\beta_{xxx} \quad \text{and} \quad C_{VV}=8/35. \tag{11e}$$

For D_3 symmetry, Kleinman symmetry implies $\beta_{xyz}=0$ and $R=0$, so with Kleinman symmetry Eqs. (11a)–(11e) reduce to the same expressions as for D_{3h} symmetry, Eqs. (9a)–(9e).

D. Molecules of C_{2V} symmetry

The molecule is taken to be in the $z-y$ plane with z the two-fold symmetry axis. There are five nonzero independent coefficients, β_{zzz}, β_{zyy}, β_{zxx}, β_{yyz}, and β_{xxz}. We assume Kleinman symmetry, which implies $\beta_{zyy}=\beta_{yyz}$ and $\beta_{zxx}=\beta_{xxz}$. Also, we assume an essentially two-dimensional structure, so that $\beta_{zxx}=\beta_{xxz}=0$. In this case Eqs. (4a)–(4c) give

$$I^{2\omega}_{\psi V} \propto \frac{1}{105}\beta^2_{zzz}[15+18R+27R^2-(24+68R+4R^2) \times \cos^2\psi+(12+48R-12R^2)\cos^4\psi], \tag{12a}$$

$$I^{2\omega}_{\psi H} \propto \frac{1}{105}\beta^2_{zzz}[3-2R+11R^2-(4+16R-4R^2)\cos^2\psi + (4+16R-4R^2)\cos^4\psi], \tag{12b}$$

$$\langle \mu_y^2 \rangle \propto \frac{1}{105}\beta^2_{zzz}[3-2R+11R^2+(-28R+28R^2)\cos^2\psi + (12+48R-12R^2)\cos^4\psi], \tag{12c}$$

$$\frac{I^{2\omega}_{VV}}{I^{2\omega}_{HV}} = \frac{15+18R+27R^2}{3-2R+11R^2}, \tag{12d}$$

where $R=\beta_{zyy}/\beta_{zzz}$ and

$$\beta_{VV}=\beta_{zzz} \quad \text{and} \quad C_{VV}=\frac{15+18R+27R^2}{105}. \tag{12e}$$

Note that when $R=-1$, Eqs. (12a)–(12e) reduce to the corresponding expressions for D_{3h} symmetry, Eqs. (9a)–(9e), as expected.[1,20] Algorithms that include the possibility of Kleinman symmetry breaking for the C_{2V} point group or groups of lower symmetry are straightforward to program. Generally, however, the equations are indeterminate as there are usually more nonzero coefficients than can reasonably be determined by HRS measurements.

V. RESULTS AND DISCUSSION

In order to calibrate the results of the HRS experiment, a reference standard is required. Carbon tetrachloride was found to be useful for this purpose as it has a reasonably large signal for a small molecule, has only one nonzero coefficient of the first hyperpolarizability, β_{xyz}, exhibits no significant absorption in the near infrared, and has been fully characterized in a previous communication.[10] This determination of β_{xyz} of CCl_4 was based on an analysis of the intra and intermolecular interactions of the molecular multipole moments and hyperpolarizabilities of CCl_4.[21,22] Of the total HRS observed from CCl_4, approximately 40% of the HRS intensity is due to the intrinsic molecular contribution from β_{xyz} for which we find a value of 19 au at 1064 nm. Preliminary results from a more direct comparison between gas phase EFISHG and HRS, liquid HRS measurements, and theoretical calculations of hyperpolarizabilities of a number of molecular liquids are in good agreement with this value for β_{xyz} of CCl_4.

Recently, Morrison *et al.*[23] address some of the difficulties that can occur regarding the use of a pure solvent such as CCl_4 as a HRS reference. These problems however, are not applicable to our experimental setup. The beam waist radius in our apparatus is ≈ 7 μm compared to ≈ 82 μm in that of Morrison *et al.* and the confocal beam length is about $260\times$ smaller. Consequently, the effective scattering source volume in our apparatus is $\approx 3000\times$ smaller than that of Morrison *et al.* and hence we are much less likely to have scattering from any residual dust in the sample. Also, the gated electronics in our photon counting apparatus accept at most one count per laser pulse, which limits the number of counts due to a possible dust scattering event. Finally, as we do a frequency scan of the scattered radiation, any residual background scattering can be subtracted off from the SHG signal.

The values of the measured first hyperpolarizabilities have long been known to be strongly dependent on the effects of the solvent on the chromophore solute.[24] This effect has also been observed in a systematic measurement of pNA in various solvents by the EFISHG experiment.[25] Due to the simplicity of the local field factors in the HRS experiment in comparison with the EFISHG measurement, an assessment of NLO chromophores in various solvents by the HRS technique should give an intrinsically more accurate means of measuring the changes in β due to different solvent conditions. The results of these measurements for the pNA molecule are collected in Table II. The value of β_{zzz} of pNA was determined through use of Eq. (6) and Eqs. (12a)–(12e). Qualitatively, the same trends observed in the EFISHG experiment are also observed in the results of the HRS experiment. However, when comparing the β values obtained from HRS experiment to those obtained from the EFISHG experiment, we find that the HRS values are $0.631\pm0.035\times$ the values obtained from the EFISHG measurement. Note, that

TABLE II. A comparison of the solvent dependence of the first hyperpolarizability β_{zzz} of pNA from the HRS measurements (referenced to β_{xyz} of CCl_4=19 au)[10] with the EFISHG measurements. The hyperpolarizabilities are given in atomic units (1 au=3.206 361×10^{-53} C^3 m^3 J^{-2}=3.6213×10^{-42} m^4 V^{-1}=8.6392×10^{-33} esu, with $\mu=1/2\ \beta E^2$). The ratio of $\beta_{zzz}^{\mathrm{HRS}}$ to $\beta_{zzz}^{\mathrm{EFISHG}}$ is nearly constant at 0.631±0.038. After adjusting this ratio by subtracting the third order hyper-polarizability contribution to the liquid EFISHG signal (≈5%) we conclude that the reference value for quartz is d_{11}=0.30±0.02 pm/V at 1064 nm. The values of the zero frequency hyper-polarizabilities, β_0, are calculated by the two-level model from the HRS measurements, except for the vapor phase results, which are extrapolated from the EFISHG measurements.

Solvent	λ_0 [nm]	$\beta_{1064}^{\mathrm{HRS}}$ [au]	$\beta_{1064}^{\mathrm{EFISHG}}$ [au]	Ratio	β_0 [au]
vapor	284		1808[a]		1201
$CDCl_3$	348	2630	3889[b]	0.676	1344
1,4 dioxane	354	2470	3774[b] 3913[c]	0.654 0.631	1225
CH_3CN	366	4430	6760[b]	0.655	2057
CH_3OD	370	4540	7408[b] 7987[d]	0.613 0.568	2061

[a]P. Kaatz and D. P. Shelton (unpublished).
[b]M. Stähelin, D. M. Burland, and J. E. Rice, Chem. Phys. Lett. **191**, 245 (1992).
[c]C. C. Teng and A. F. Garito, Phys. Rev. B **28**, 6766 (1983).
[d]J. L. Oudar and D. S. Chemla, J. Chem. Phys. **66**, 2664 (1977).

the EFISHG determination of β for pNA is also typically ≈5% too large due to neglect of the third order contribution [recall Eq. (1)]. As the reference standard used in the EFISHG experiments was a quartz crystal with an assumed SHG coefficient of d_{11}=0.5 pm/V, our results from the HRS experiment imply that the quartz reference value should be d_{11}=0.30±0.02 pm/V. This value is in agreement with the conclusions of Roberts,[26] recent measurements by Mito *et al.*[27] and also with an earlier determination by Levine and Bethea.[28]

As has been noted previously, many chromophores of interest for applications in nonlinear or electro-optics also exhibit a large two-photon induced fluorescence effect.[8] In fact, many of the chromophores listed in Table I are also used as laser dyes and/or fluorescent probes. Previous authors have overestimated the values for β obtained from HRS measurements, as the two-photon induced fluorescence typically overlaps with the HRS spectrum to a significant extent.[8,29] This is illustrated in Fig. 3 for the DANS chromophore for HRS with excitation at a fundamental wavelength of 1064 nm. For comparison, HRS from pNA is also shown in Fig. 3, from which there is a negligible amount of two-photon induced fluorescence. Evidence that this is a two-photon process in shown in Fig. 4 which illustrates the power dependence of the fluorescence for the case of DANS near the two-photon fluorescence emission maximum at 16500 cm^{-1} (606 nm). The power law coefficient of m=2.02 indicates that the fluorescence is excited by a two-photon absorption process. The results from the other chromophores

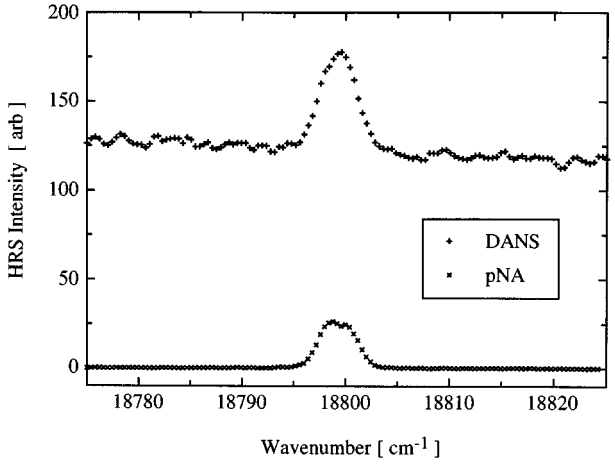

FIG. 3. The HRS spectrum in the VV scattering geometry of pNA (0.083 M) and DANS (9.3×10^{-4} M) in 1,4 dioxane with excitation at a fundamental wavelength of 1064 nm. The spectral slit width was 2.2 cm^{-1}. The background two-photon fluorescence intensity is approximately linear in a small spectral region near the second harmonic peak at 18797 cm^{-1}. Subtracting off the background provides a correct measurement of the contribution of the first hyperpolarizability to the HRS spectrum.

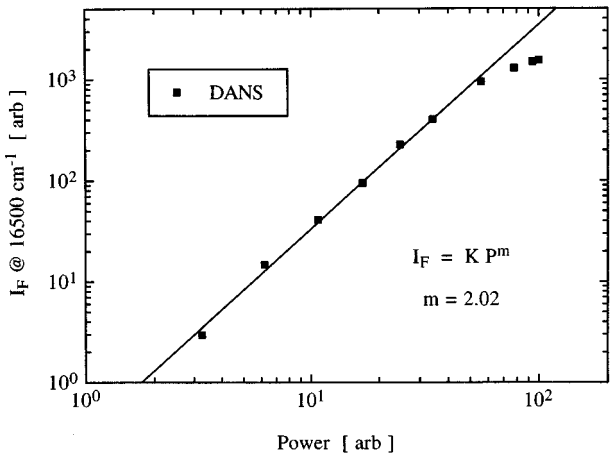

FIG. 4. Power dependence of the two-photon induced fluorescence intensity, I_F, at 16500±2.2 cm^{-1} (606 nm), which is near the fluorescence intensity maximum of DANS with irradiation at 1064 nm. The coefficient m=2.02 indicates a two-photon absorption process. The curve rolls over at high intensity due to thermal lensing of the incident beam.

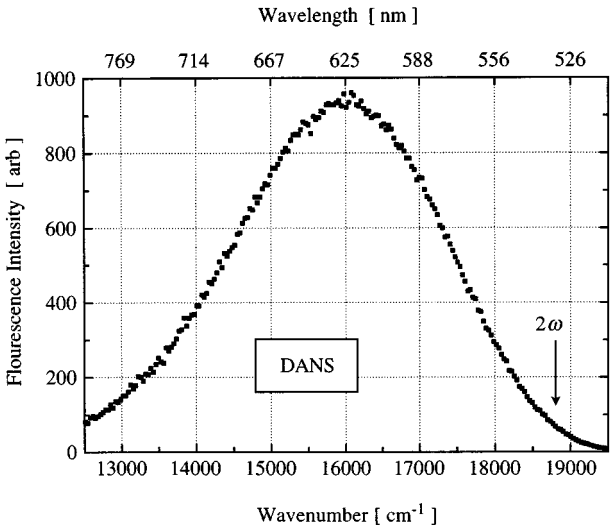

FIG. 5. The spectrum of the two-photon induced fluorescence from DANS with irradiation at 1064 nm. The spectrum is similar to the single-photon-induced fluorescence spectrum. The measured spectrum is corrected for the spectral response of the spectrometer, see Fig. 2. The HRS peak at $2\omega = 18797\ \mathrm{cm}^{-1}$ seen in Fig. 3 is undetectable here because of the low spectral resolution.

exhibiting two-photon fluorescence are similar. The two-photon fluorescence spectrum obtained by excitation at 1064 nm is shown for the DANS chromophore in Fig. 5. At this level of resolution, the second harmonic scattered light is lost in the two-photon induced fluorescence background. The two-photon fluorescence has the same spectral profile as observed from the single-photon fluorescence spectrum.

Separation of the second harmonic signal from the two-photon induced fluorescence depends on the location of the second harmonic frequency with regard to the emission maximum of the two-photon induced fluorescence and their relative integrated intensities. These values are indicated in Tables III and IV along with the values for the first hyperpolarizabilities derived from the HRS measurement. Resolving the HRS peak from the two-photon induced fluorescence, as shown in Fig. 3, requires long or multiple scans over a narrow frequency range near the second harmonic. Doing the HRS experiment at longer excitation wavelengths, does not always alleviate the problem of the two-photon induced fluorescence background. Even with excitation at 1319 nm DANS and other chromophores exhibit a non-negligible light scattering contribution from the two-photon induced fluores-

TABLE III. Optical and nonlinear optical properties of selected chromophores at $\lambda_\omega = 1064$ nm. See Table I for a listing of the chromophore acronyms. The absorption maximum and the two-photon induced fluorescence maximum are given by λ_0 and λ_F, respectively. The integrated two-photon induced fluorescence intensity (photon flux) and the integrated HRS intensity are indicated by I_F and I_{HRS}. The uncertainty in the measured depolarization ratio of $I_{VV}^{2\omega}/I_{HV}^{2\omega}$ is in the range of 2%–3%. The ratio of hyperpolarizability components R is obtained by inverting the expression for the polarization ratio as a function of R. Figure 6 shows a graph of Eq. (12d) which expresses this relation in the case of C_{2V} symmetry. The uncertainty of R depends on the slope of the graph and for values of $I_{VV}^{2\omega}/I_{HV}^{2\omega} \approx 5$ the relative uncertainty of R is approximately ± 0.015 (see the inset of Fig. 6). Absolute values of the first hyperpolarizability β were obtained by comparison with β_{xyz} of CCl_4, which has a value of 19 au at $\lambda_\omega = 1064$ nm (Ref. 10). Values for the first hyperpolarizabilities β are given in relative units (relative to β_{zzz} of pNA) and absolute atomic units (au) (see Table II for a list of conversion factors to other units). The zero frequency hyperpolarizability, β_0, is calculated by the two-level model from the measurements at 1064 nm.

Chromophore	Group	λ_0 [nm]	λ_F [nm]	I_F/I_{HRS}	$1/C_{VV}$	$I_{VV}^{2\omega}/I_{HV}^{2\omega}$	R	β_{HRS}^{1064}	β_{HRS}^{1064} [au]	β_0 [au]
pNA	C_{2V}	354		<2	7.1	4.9	−0.008	1	2 470	1 225
oNA	C_s	370			5.8,3.0[a]	6.1	+0.14,+0.60	0.2–0.3	620	300
mNA	C_s	397						≈0.15	370	150
DAB	C_{2V}	329			6.6	5.5	+0.048	0.82	2 020	1 100
MNA	C_{2V}	361	610	30	6.5	5.6	+0.060	0.92	2 270	1 090
DAC	C_{2V}	371	600	100	6.8	5.2	+0.018	2.9	7 260	3 280
MK	C_{2V}	322			8.7	2.7	−0.280	0.85	2 100	1 220
DBCP	C_{2V}	345, 359s[b]			8.7	2.5	−0.330	0.60	1 480	750
BDABA	C_{2V}	426	550	950	8.5	3.0	−0.230	5.3	13 100	3 960
DABMN	C_{2V}	420	630	10	7.3	4.7	−0.033	4.8	11 800	3 760
DANS	C_{2V}	426	625	25 000	6.9	5.1	+0.015	14	34 600	10 400
Coumarin 334	C_{2V}	438	620	200	7.6	4.3	−0.070	4.7	11 700	3 130
DCM	C_{2V}	455	560	28 000	6.4	5.6	+0.073	19	46 900	10 300
DR1	C_{2V}	474	640	20	6.8	5.2	+0.021	33	81 500	13 400
LDS 722	C_{2V}	489	650	33 000	7.1	4.9	−0.013	50	123 000	15 100
Styryl 7	C_{2V}	563	700	190 000	7.5	4.4	−0.065	92	227 000	10 600
DIA	C_{2V}	566		<2	7.0	5.0	+0.002	19	46 900	4 400
RB	C_{2V}	562	590	71 000				≈12	29 600	2 400
CV	D_3	589		5	4.4	1.5		27	66 700	10 400
BG	C_{2V}	632			7.6	2.1	−0.300[c]	17	42 000	11 200
BTB (acid)[d]	C_1	420			7.6	4.3	−0.072	2.5	6 160	1 960
BTB (base)[d]	C_1	613			7.5	4.4	−0.062	26	64 200	14 100

[a]The polarization data for oNA can be fit assuming C_{2V} symmetry with $R = +0.14$ or $+0.60$. See Fig. 9 and the related discussion.
[b]Shoulder at 359 nm.
[c]The polarization data for BG cannot be fitted assuming Kleinman symmetry at 1064 nm. See Fig. 7 and the related discussion.
[d]The polarization data for BTB is fitted assuming C_{2V} symmetry.

TABLE IV. Optical and nonlinear optical properties of selected chromophores at λ_ω=1319 nm. See Table I for a listing of the chromophore acronyms. The remaining notation is the same as that used in Table III. Absolute values of the first hyperpolarizability were obtained by comparison with β_{xyz} of CCl_4 which was assumed to have a value of 18 au at λ_ω 1319 nm. Values for the first hyperpolarizabilities β are given in units to β_{zzz} of pNA and absolute atomic units (au), see Table II for conversion factors to other commonly used units. The zero frequency hyperpolarizability, β_0, is calculated by the two-level model from the measurements at 1319 nm.

Chromophore	Group	λ_0 [nm]	λ_F [nm]	I_F/I_{HRS}	$1/C_{VV}$	$I^{2\omega}_{VV}/I^{2\omega}_{HV}$	R	β^{HRS}_{1319}	β^{HRS}_{1319} [au]	β_0 [au]
pNA	C_{2V}	354		<2	6.5	5.6	+0.063	1	1 850	1 225
DABMN	C_{2V}	420			6.5	5.5	+0.058	3.8	7 030	3 760
DANS	C_{2V}	426	620	430	6.8	5.2	+0.026	8.8	16 300	8 520
DCM	C_{2V}	455	740	1 000	7.2	4.8	−0.022	10.5	19 400	8 960
DR1	C_{2V}	474		<2	6.8	5.2	+0.025	13.3	24 600	10 400
LDS 722	C_{2V}	489	710	600	7.1	4.9	−0.009	25	46 300	18 000
Styryl 7[a]	C_{2V}	563	705							
DIA	C_{2V}	566		<2	7.0	5.0	+0.006	23	42 600	9 150
CV	D_3	589		7	4.4	1.5		16	29 600	4 800
BG	C_{2V}	632			8.7	2.4	−0.340	58	107 000	6 730
BTB (base)[b]	C_1	613			7.4	4.5	−0.048	24	44 400	4 740

[a]The HRS at 1319 nm from Styryl 7 is masked by the intense two-photon induced fluorescence.
[b]The polarization data for BTB is fitted assuming C_{2V} symmetry.

cence. And in the extreme case of Styryl 7 with excitation at 1319 nm, it is not even possible to separate the contribution of the two-photon induced fluorescence from the scattered second harmonic light with our apparatus.

Also indicated in Tables III and IV are the extrapolated zero frequency values of the first hyperpolarizabilities obtained by applying the two-level model to the HRS measurements at 1064 and 1319 nm. The two level model can be described in terms of the transition frequency, ω_{eg}, (the corresponding wavelength λ_0 is given in Tables III and IV) of the highest occupied-lowest unoccupied energy level transition.[4,30] The frequency response of β can then be modeled as

$$\beta(-2\omega,\omega,\omega)=\frac{\omega_{eg}^4}{(\omega_{eg}^2-4\omega^2)(\omega_{eg}^2-\omega^2)}\,\beta_0, \tag{13}$$

where β_0 is given by

$$\beta_0=\frac{3}{2\epsilon_0 h^2}\,\frac{\Delta\mu\cdot\mu_{eg}^2}{\omega_{eg}^2}. \tag{14}$$

The difference between excited and ground state electric dipole moments is given by $\Delta\mu$ and μ_{eg} is the transition dipole moment between the ground and excited state. We estimate β_0 using the two-level model by substituting the measured values of β, λ, and λ_0 into Eq. (13).

The values for β_0 of pNA in selected solvents are also tabulated in Table II. The two-level model predicts an approximate second order dependence of β_0 with λ_0, from Eq. (14). This power law prediction has generally been verified in studies of the relationship of β with respect to the conjugation dependencies (length) of different chromophores.[31–33] The β_0 value implied from our HRS results, however, indicates that pNA in 1,4 dioxane gives within experimental error the same β_0 value as the vapor phase EFISHG measurement of pNA, whereas the two-level model predicts that β_0 should increase by ≈40%. The values for β_0 of pNA in more polar solvents such as acetonitrile (CH_3CN) or methanol (CH_3OD) are in approximate agreement with the two-level model prediction of an ≈70% increase of β_0 with respect to the corresponding value obtained from the vapor phase EFISHG measurement. These HRS results are in agreement with the previous EFISHG measurements.[25]

The adequacy of the two-level model for a constant chromophore/solvent system can be assessed by comparing the corresponding β_0 values in Tables III and IV. In general, we find that the two-level model adequately describes the measured increase in β as the incident wavelength decreases from 1319 to 1064 nm for the single ring systems such as pNA, as the agreement in β_0 from Tables III and IV indicates. For the larger two ring or central atom systems however, the value of β_0 obtained from a measurement at 1064 nm typically provides an unreliable prediction of the value of β obtained from a measurement at 1319 nm.

The results of Tables III and IV are generally in reasonable agreement with the EFISHG results on the same molecules. Occasionally, however, there are significant differences. For example, after correcting for the differences in the definition of β, quartz reference value (d_{11}), and accounting for dispersion via the two level model, we obtain nearly the same value for β_{zzz} of DANS by the HRS measurement as do Cheng *et al.*[5] by the EFISHG experiment. In comparing the same measurements of DR1, however, the results of Cheng *et al.* are 53% lower than our HRS measurements. For DR1, the HRS measurements at 1319 nm are not expected to be resonantly enhanced, so the two measurement procedures should yield equivalent values for β_0 but they do not. Such discrepancies can lead to large differences in the measured values of β from various groups, as the EFISHG results have occasionally been used to calibrate the results from HRS measurements.[34–37]

Most of the chromophores investigated in this work have at least quasi C_{2V} symmetry. The nonlinear optical properties of these chromophores have traditionally been assumed to be one-dimensional, primarily because the EFISHG experiment is incapable of assessing the relative magnitude of hyperpolarizability components. In contrast, HRS measurements are

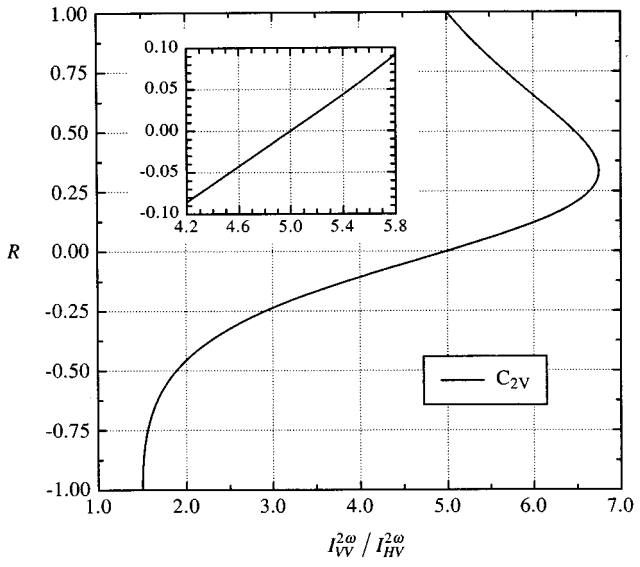

FIG. 6. The value of $R=\beta_{zyy}/\beta_{zzz}$ for C_{2V} symmetry as a function of the measured polarization ratio, $I^{2\omega}_{\mathrm{VV}}/I^{2\omega}_{\mathrm{HV}}$, as calculated from Eq. (12d). Most of the molecules in Tables III and IV have approximately C_{2V} symmetry with a polarization ratio $I^{2\omega}_{\mathrm{VV}}/I^{2\omega}_{\mathrm{HV}}$ in the range of 4.2–5.8. The inset shows that the relation between the polarization ratio and values of R obtained from Eq. (12d) are approximately linear in this range. Although in principle, R is double valued for measured values of $I^{2\omega}_{\mathrm{VV}}/I^{2\omega}_{\mathrm{HV}}>5$, most of the molecules with C_{2V} symmetry investigated in this work have a strong charge transfer axis. The component of the first hyperpolarizability along this axis, β_{zzz}, is expected to dominate the nonlinear response. Exceptions are the ''lambda'' molecules, for which $R\approx-0.30$.

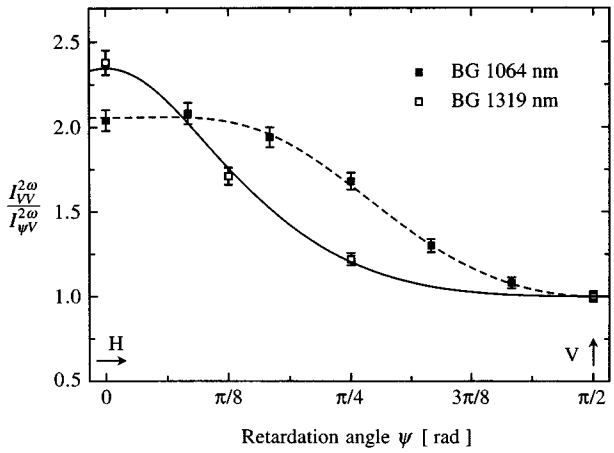

FIG. 7. The measured polarization ratios $I^{2\omega}_{\mathrm{VV}}/I^{2\omega}_{\psi\mathrm{V}}$ of BG with irradiation at 1064 nm (solid squares) and at 1319 nm (open squares) as a function of the retardation angle ψ. At 1319 nm, the polarization data can be fitted assuming Kleinman symmetry for a molecule of C_{2V} symmetry with $R=-0.340$ (solid curve). At 1064 nm, however, where the second harmonic occurs in the absorption band of the molecule, the data cannot be fitted assuming Kleinman symmetry. The dashed curve through the data at 1064 nm is drawn assuming C_{2V} symmetry with parameter values $\beta_{zyy}/\beta_{zzz}=\beta_{yyz}/\beta_{zzz}=-0.300$, $\beta_{zxx}/\beta_{zzz}=+0.330$, and $\beta_{xxz}/\beta_{zzz}=0$. The fit at 1064 nm is optimized assuming that the values for β_{zyy} and β_{yyz} change relatively little from their values at 1319 nm (see text).

able to give some insight into the magnitude of other components. Figure 6 shows the dependence of the ratio $R=\beta_{zyy}/\beta_{zzz}$ as a function of the measured polarization ratio $I^{2\omega}_{\mathrm{VV}}/I^{2\omega}_{\mathrm{HV}}$ for the case of C_{2V} symmetry. As can be seen in Tables III and IV, for molecules of C_{2V} symmetry R is usually less than 10%, verifying the hypothesis generally assumed in EFISHG measurements.

Interesting exceptions are the ''lambda'' (donor–acceptor–donor) chromophores, such as MK, DBCP, BDABA, and BG, for which R is ≈-0.30. There has been recent interest in these chromophores for applications involving both NLO crystals and poled polymers.[38–40] The results of the HRS polarization measurements of BG at 1064 and 1319 nm are shown in Fig. 7. At 1319 nm the results indicate that Kleinman symmetry is valid. However, at 1064 nm, we are unable to fit the polarization data assuming Kleinman symmetry. The HRS polarization data at 1064 nm are fit assuming C_{2V} symmetry with parameter values $\beta_{zyy}/\beta_{zzz}=\beta_{yyz}/\beta_{zzz}=-0.300$, $\beta_{zxx}/\beta_{zzz}=+0.330$, and $\beta_{xxz}/\beta_{zzz}=0$. As the second harmonic falls within the absorption band of BG, the breaking of Kleinman symmetry might be expected, although this does not appear to be universally true, as the HRS measurements of, for example, Styryl 7 and DIA at 1064 do not indicate any significant deviation from Kleinman symmetry. The fits at 1319 and 1064 nm are optimized with a minimal set of hyperpolarizability parameters that satisfy the polarization data. Thus at 1319 nm, the assumption of Kleinman symmetry of a 2D C_{2V} molecular structure is sufficient to fit the data. For the subsequent fit of the data at 1064 nm, the hyperpolarizability values for β_{zyy} and β_{yyz} are assumed to change relatively little from their values at 1319 nm. Less restrictive assumptions regarding the hyperpolarizability components are also able to satisfy the polarization data. However, when the preceding assumptions are relaxed, the fits do not converge to a unique solution due to the weak functional dependence of the hyperpolarizability components on the polarization ratios.

The crystal violet (CV) cation has been proposed as a prototypical case of a NLO molecule with octupolar symmetry.[2,37,41] In solution, the CV cation is usually assumed to have the shape of a symmetric D_3 propeller, where the three aromatic rings are rotated out of the molecular plane by 30°, although suggestions of a possible rotational isomer with C_2 symmetry have also been proposed.[42–44] Previous HRS measurements have further assumed that the CV molecule has D_{3h} symmetry. The analysis from Eqs. (9a), (9e), (11a), and (11e) indicates that unless Kleinman symmetry is invalid, the polarization results for a molecule of D_3 symmetry will be indistinguishable from those for the D_{3h} point group. Our HRS polarization measurements at both 1064 (as indicated in Fig. 8) and 1319 nm are not able to reveal any deviation from Kleinman symmetry for β of CV. The HRS polarization results imply that even if the CV molecule does have the D_3 propeller symmetry, that $R=0.00\pm0.15$. Therefore, the HRS polarization measurements at 1064 and 1319 nm are unable to determine whether the CV cation has D_3 or D_{3h} symmetry.

A number of different HRS measurements have been

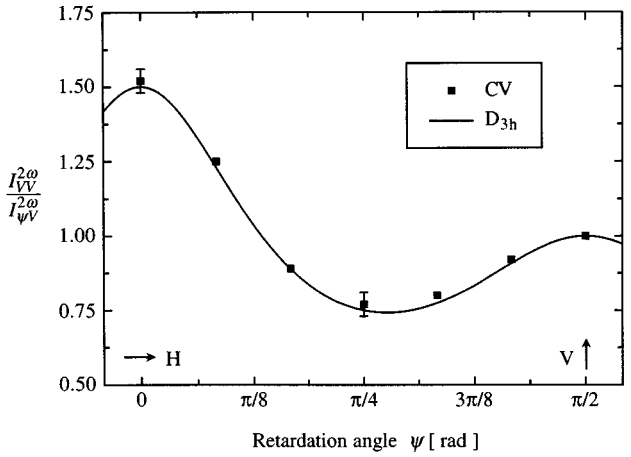

FIG. 8. The measured polarization ratios $I_{VV}^{2\omega}/I_{\psi V}^{2\omega}$ of CV with irradiation at 1064 nm (solid squares) as a function of the retardation angle ψ. The curve shows that the HRS polarization data can be fit assuming CV has D_{3h} symmetry, or equivalently, assuming D_3 symmetry with $R=\beta_{xyz}/\beta_{xxx}=0.0\pm0.15$. The HRS polarization results from irradiation at 1319 nm are similar.

reported for the CV molecule, with widely different results.[2,23,37,41,45] Our own results off resonance at 1319 nm compare best with the long wavelength measurements of Stadler *et al.*[37] At 1319 nm we obtain a value for β_{yyy} of CV that is $1.20\times\beta_{zzz}$ of DR1, while Stadler *et al.* find a value of $1.35\times\beta_{zzz}$ of DR1 at 1500 nm. We disagree on the absolute value of DR1, however, for reasons discussed previously. The possibility of residual scattering as discussed by Morrison *et al.*[23] may explain the difference in the results as Stadler *et al.* use an unfocused beam in their HRS apparatus, which provides a much larger scattering source volume. The results at other wavelengths likely involve differences in accounting for absorption, excess scattering, and/or the method used to infer a β value.

For reasons of symmetry, both the ground and excited state dipole moments are identically zero for octupolar molecules. Thus the two-level model is not applicable to these molecules, as is evident from Eq. (14). The β_0 values in Tables III and IV for CV are obtained from a three-level model with nearly degenerate excited states.[41] The frequency dependence of β for this model is exactly the same as the two-level model result given by Eq. (13). At 1064 nm the measured β value of CV is comparable to that of DR1. However, as indicated previously, the resonantly enhanced value of β from the HRS measurement at 1064 nm provides an unreliable prediction of the value of β_0, as this value of β_0 is more than twice as high as the value for β_0 derived from the HRS measurement at 1319 nm.

A number of theoretical calculations exist for hyperpolarizability components of pNA.[46–49] Some of these calculations are collected in Table V and compared with our HRS and EFISHG measurements. In general, the calculated polarization ratios, $I_{VV}^{2\omega}/I_{HV}^{2\omega}$, are significantly lower than our measured ratios. Moreover, we find that there is considerable dispersion in β_{zyy} for pNA. At 1064 nm we find $R=-0.008\pm0.015$, while at 1319 nm $R=+0.063\pm0.015$. The results of the HRS measurements at 1064 nm are shown in Fig. 9 with the corresponding fit to C_{2V} symmetry using Eqs. (12a)–(12e).

The polarization ratio $I_{VV}^{2\omega}/I_{VH}^{2\omega}$ of pNA measured at 1064 nm in this work is significantly higher (about 9%) than previous results.[35,50] Lower values obtained by previous authors may be partly due to a neglect of the effect of the finite aperture of the collection optics used in the apparatus of their HRS experiments. As an indication of the size of such effects with the apparatus used in this work, the uncorrected measured polarization ratio $I_{VV}^{2\omega}/I_{HV}^{2\omega}$ is predicted to be about 8% smaller than the uncorrected measured $I_{VV}^{2\omega}/I_{HV}^{2\omega}$ polarization ratio for pNA, whereas, the corrected polarization ratios must be equal. This was experimentally verified for pNA at both incident wavelengths (1064 and 1319 nm). As this finite aperture effect is more important for larger HRS polarization ratios, a comparison of HRS measurements with other ''stan-

TABLE V. Experimental and theoretical first hyperpolarizability components of pNA.

Method	λ_ω [nm]	β_{zzz} [au]	β_{zxx} [au]	β_{zyy} [au]	β_z [au]	$I_{VV}^{2\omega}/I_{HV}^{2\omega}$	Ref.
EFISHG[a]	1064				1808		
EFISHG[b]	1319				1546		
EFISHG[b]	∞				1201		
HRS[c]	1064	2470	0	−20	2450	4.9±0.1	
HRS[c]	1319	1850	0	+117	1967	5.6±0.1	
HRS[c]	∞	1225[b]					
CNDO	1064	1999	−1	−492	1506	4.24	46
HF	1064	1715	−28	−256	1431	3.55	47
HF	1370	1500	−27	−236	1237	3.47	47
AM1		2702	0	−447	2255	3.51	48
3-21G		2211	0	−384	1827	3.45	48
INDO		1975	0	−14	1961	4.93	48
HF	∞	635	−24	−95.6	515	3.40	49
MP2	∞	1029	−23	−39	967	4.44	49

[a]Results from a vapor phase EFISHG measurement.
[b]Extrapolated by the two-level model using the vapor phase measurement at 1064 nm.
[c]Results from measurement in 1,4 dioxane.

TABLE VI. Experimental and theoretical first hyperpolarizability components of oNA.

Method	λ_ω [nm]	β_{zzz} [au]	β_{yyy} [au]	β_{zzy} [au]	β_{zyy} [au]	β_z [au]	R	$I_{VV}^{2\omega}/I_{HV}^{2\omega}$	Ref.
HRS[a]	1064	709	0	0	+100	809	+0.14	6.1±0.1	
HRS[a]	1064	510	0	0	+306	816	+0.60	6.1±0.1	
EFISHG[a]	1907					404[b]			5
INDO		1313	132	−360	235	1560	+0.18	5.3	51

[a]Results from measurement in 1,4 dioxane.
[b]For comparison with the HRS measurements, the extrapolated value (2-level model) of β_z is 730 au at 1064 nm.

dard'' NLO chromophores of C_{2V} symmetry may prove useful to resolve these discrepancies.

A comparison between the results of HRS measurements and theoretical calculations of Shuai *et al.*[51] for oNA are given in Table VI. The corresponding HRS polarization measurements are also shown in Fig. 9. Although oNA does not have C_{2V} symmetry, the HRS results can be fit quite well by Eqs. (12a)–(12e), where both $R=+0.14$ or $R=+0.60$ are consistent with $I_{VV}^{2\omega}/I_{HV}^{2\omega}=6.1$. For comparison with the calculations of Shuai *et al.* we have assumed the same molecular coordinate system which indicates that the largest hyperpolarizability component is given by β_{zzz}, as the HRS measurements are incapable of distinguishing between β_{zzz} and β_{yyy} (the z-axis is along the donor-substituent axis, with y perpendicular to z and in the plane of the benzene ring). With this assumption, the theoretical calculations indicate that $R=+0.18$, with however, other nonzero coefficients. These other coefficients contribute to a predicted depolarization ratio, $I_{VV}^{2\omega}/I_{HV}^{2\omega}=5.3$, which should be compared to the measured value of 6.1 ± 0.1. For the case of oNA and the other molecules of low symmetry, more generalized polarization geometries may prove useful in determining the relevant hyperpolarizability components.[16,17]

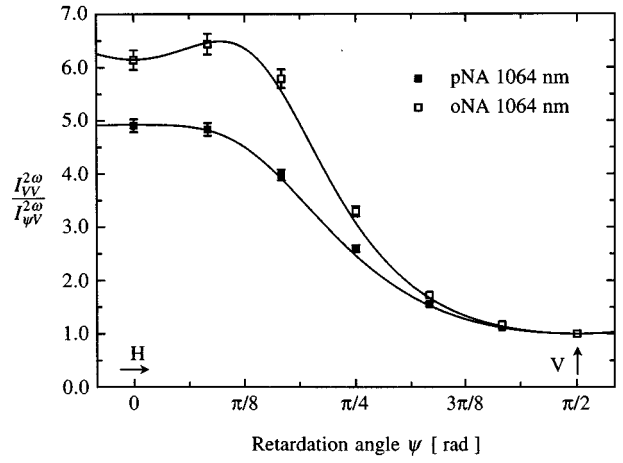

FIG. 9. The measured polarization ratios $I_{VV}^{2\omega}/I_{\psi V}^{2\omega}$ obtained from HRS (incident radiation at 1064 nm) of pNA (solid squares) and oNA (open squares) as a function of the retardation angle ψ. The polarization data for pNA can be uniquely fitted with $R=-0.008\pm0.015$. Although oNA does not have C_{2V} symmetry, the polarization data can be fitted with Eqs. (12a–12e) equally well with $R=+0.14\pm0.02$ or $R=+0.60\pm0.02$. The two curves are indistinguishable and both give $I_{VV}^{2\omega}/I_{HV}^{2\omega}=6.1$.

VI. CONCLUSIONS

In contrast to previous work on HRS measurements from NLO chromophores, we find it essential to incorporate a scanning monochromator to analyze the properties of the scattered light. Quite often molecules of interest for nonlinear optical and electro-optic applications also exhibit two-photon induced fluorescence that can interfere with the analysis of the second harmonic scattered light. Interference filters are usually inadequate for selecting just the second harmonic photons. The existence of the strong two-photon induced fluorescence in many of these chromophores also has implications for potential SHG devices, as prolonged two-photon induced fluorescence usually leads to eventual bleaching of the NLO chromophores.[52,53]

The HRS technique is a useful alternative to the well-established EFISHG measurement for the determination of the molecular β of NLO chromophores. The HRS measurement generally provides more information on a number of independent β components and is also applicable to molecular salts and molecules of low symmetry. The EFISHG experiment does have advantages for the measurement of chromophores that absorb far into the red, however. We find that the HRS measurement yields results for β that are generally consistent with the previous EFISHG measurements, provided that the NLO susceptibility of the quartz reference typically used to calibrate these measurements is taken to be $d_{11}=0.30\pm0.02$ pm/V.

[1] J. Zyss and I. Ledoux, Chem. Rev. **94**, 77 (1994).
[2] T. Verbiest, K. Clays, C. Samyn, J. Wolff, D. Reinhoudt, and A. Persoons, J. Am. Chem. Soc. **116**, 9320 (1994).
[3] A. Willetts, J. E. Rice, D. M. Burland, and D. P. Shelton, J. Chem. Phys. **97**, 7590 (1992).
[4] C. Bosshard, K. Sutter, P. Prêtre, J.-Hulliger, M. Floörsheimer, P. Kaatz, and P. Günter, *Organic Nonlinear Optical Materials* (Gordon and Breach, Basel, 1995).
[5] L.-T. Cheng, W. Tam, S. H. Stevenson, G. R. Meredith, G. Rikken, and S. R. Marder, J. Chem. Phys. **95**, 10631 (1991).
[6] D. P. Shelton, Phys. Rev. A **42**, 2578 (1990).
[7] M. Stähelin and I. Zschokke-Gränacher, Nonlinear Optics **9**, 241 (1995).
[8] M. C. Flipse, R. Jonge, R. H. Woudenberg, A. W. Marsman, C. Walree, and L. W. Jenneskens, Chem. Phys. Lett. **245**, 297 (1995).
[9] S. Stadler, G. Bourhill, and C. Bräuchle, J. Phys. Chem. **100**, 6927 (1996).
[10] P. Kaatz and D. P. Shelton, Mol. Phys. **88**, 683 (1996).
[11] R. W. Terhune, P. D. Maker, and C. M. Savage, Phys. Rev. Lett. **14**, 681 (1965).
[12] P. D. Maker, Phys. Rev. A **1**, 923 (1970).
[13] P. Kaatz and D. P. Shelton, Rev. Sci. Instrum. **67**, 1438 (1996).
[14] R. Bersohn, Y. H. Pao, and H. L. Frisch, J. Chem. Phys. **45**, 3184 (1966).
[15] S. J. Cyvin, J. E. Rauch, and J. C. Decius, J. Chem. Phys. **43**, 4083 (1965).
[16] W. M. McClain, J. Chem. Phys. **57**, 2264 (1972).

[17] M. Kauranen and A. Persoons, J. Chem. Phys. **104**, 3445 (1996).
[18] A. Yariv and P. Yeh, *Optical Waves in Crystals* (Wiley, New York, 1984).
[19] P. N. Butcher and D. Cotter, *The Elements of Nonlinear Optics* (Cambridge University Press, Cambridge, 1990).
[20] J. Zyss, J. Chem. Phys. **98**, 6583 (1993).
[21] S. Kielich, Acta Phys. Polon. **33**, 89 (1968).
[22] S. Kielich, and M. Kozieŀowski, Acta Phys. Polon. A **45**, 231 (1974).
[23] I. D. Morrison, R. G. Denning, W. M. Laidlaw, and M. A. Stammers, Rev. Sci. Instrum. **67**, 1445 (1996).
[24] A. T. Amos and B. L. Burroughs, in *Adv. Quant. Chem.* 7, edited by P. O. Löwdin (Academic, New York, 1973), p. 289.
[25] M. Stähelin, D. M. Burland, and J. E.-Rice, Chem. Phys. Lett. **191**, 245 (1992).
[26] D. A. Roberts, IEEE J. Quant. Elect. QE **28**, 2057 (1992).
[27] A. Mito, K. Hagimoto, and C. Takahashi, Nonlinear Optics **13**, 3 (1995).
[28] B. F. Levine and C. G. Bethea, Appl. Phys. Lett. **20**, 272 (1971).
[29] H. Nakanishi, X.-M. Duan, S. Okada, H. Oikawa, and M. Matsuda, in *Organic Thin Films for Photonics Applications*, **21** OSA Technical Digest Series (Optical Society of America, Portland OR, 1995), p. 268.
[30] J. L. Oudar and D. S. Chemla, J. Chem. Phys. **66**, 2664 (1977).
[31] A. Dulcic, C. Flytzanis, C. L. Tang, D. Pepin, M. Fetizon, and Y. Hoppolliard, J. Chem. Phys. **74**, 1559 (1981).
[32] L.-T. Cheng, W. Tam, S. H. Stevenson, S. R. Marder, A. E. Stiegman, G. Rikken, and C. W. Spangler, J. Phys. Chem. **95**, 10643 (1991).
[33] K. Y. Wong, A. K. Y. Jen, and V. Pushkara Rao, Phys. Rev. A **49**, 3077 (1994).
[34] K. Clays and A. Persoons, Phys. Rev. Lett. **66**, 2980 (1991).
[35] G. J. T. Heesink, A. G. T. Ruiter, N. F. van Hulst, and B. Bölger, Phys. Rev. Lett. **71**, 999 (1993).
[36] M. A. Pauley, C. H. Wang, and A. K. Y. Jen, J. Chem. Phys. **102**, 6400 (1995).
[37] S. Stadler, R. Dietrich, G. Bourhill, and C. Bräuchle, Opt. Lett. **21**, 251 (1996).
[38] S. Genbo, G. Shouwu, P. Feng, H. Youping, and L. Zhengdong, J. Phys. D: Appl. Phys. **26**, B236 (1993).
[39] J. Kawamata, K. Inoue, and T. Inabe, Appl. Phys. Lett. **66**, 2102 (1995).
[40] S. Ermer, S. M. Lovejoy, and D. S. Leung, in *Polymers for Second Order Nonlinear Optics*, edited by G. A. Lindsay and K. D. Singer (ACS Symp. Series, **601**, Washington, DC, 1995), p. 95.
[41] J. Zyss, T. C. Van, C. Dhenaut, and I. Ledoux, Chem. Phys. **177**, 281 (1993).
[42] H. P. Dekkers and E. C. Kielman-van Luyt, Mol. Phys. **31**, 1001 (1976).
[43] H. B. Lueck, J. L. McHale, and W. D. Edwards, J. Am. Chem. Soc. **114**, 2342 (1992).
[44] H. B. Lueck, D. C. Daniel, and J. L. McHale, J. Raman Spect. **24**, 363 (1993).
[45] O. F. J. Noordman and N. F. van Hulst, Chem. Phys. Lett. **253**, 145 (1996).
[46] S. J. Lalama and A. F. Garito, Phys. Rev. A **20**, 1179 (1979).
[47] S. P. Karna, P. N. Prasad, and M. Dupuis, J. Chem. Phys. **94**, 1171 (1991).
[48] J. L Brédas, F. Meyers, B. M. Pierce, and J. Zyss, J. Am. Chem. Soc. **114**, 4928 (1992).
[49] F. Sim, S. Chin, M. Dupuis, and J. E. Rice, J. Phys. Chem. **97**, 1158 (1993).
[50] T. Verbiest, M. Kauranen, and A. Persoons, J. Chem. Phys. **101**, 1745 (1994).
[51] Z. Shuai, S. Ramasesha, and J. L. Brédas, Chem. Phys. Lett. **250**, 14 (1996).
[52] R. A. Norwood, D. R. Holcomb, and F. F. So, J. Nonlinear Opt. **6**, 193 (1993).
[53] M. Cha, W. E. Torruellas, G. I. Stegeman, W. H. G. Horsthuis, G. R. Möhlmann, and J. Meth. Appl. Phys. Lett. **65**, 2648 (1994).